Investigation of Magnetohydrodynamic Flight Control

WILLIAM B. ERICSON* AND ALGIRDAS MACIULAITIS†
Grumman Aircraft Engineering Corporation, Bethpage, L. I., N. Y.

This report presents the results of an investigation into the use of a magnetic field in the nose region of a hypersonic vehicle as a means of flight control. The vehicle is assumed to be moving at speeds that cause shock-ionization of a significant portion of the shock layer. The altitude-speed regimes in which this ionized flow will strongly interact with a magnetic field are determined. The governing interaction parameter Q' is essentially based on the shock standoff distance. The magnetohydrodynamic control forces, which can be generated within these large interaction regimes ($Q' > 1$), are computed. It is shown that the critical portion of a typical flight path (down to 30 km and 6 km/sec) for interplanetary reentry lies well within the MHD control regime.

Nomenclature

A_b = frontal cross-sectional area of body nose, m²
$\mathbf{B}$ = magnetic induction, Weber/m²
B_0 = value of magnetic induction at stagnation point, Weber/m²
$\mathbf{E}$ = electric field, v/m
f = fraction of nonionized atoms $n_0/(n_0 + n_e)$
f_M = dimensionless value of F_M
F_M = control force due to applied B field, N
j = electric current density, amp/m²
k = Hall current parameter
p = Δ/r_b, nondimensional shock detachment distance, or pressure, N/m²
q = dynamic pressure $\frac{1}{2}\rho u^2$, N/m²
Q' = $(1/A_b)\int_\tau(\sigma_{\text{eff}}B^2/\rho_\infty u_\infty)d\tau$ magnetic interaction parameter
r = radius, or radial coordinate, m
$\mathbf{u}$ = fluid velocity, m/sec
$\bar{u}_\alpha$ = average value of crossflow velocity through magnetic field, m/sec
α = angle of attack of the magnetic field centerline with respect to freestream, deg
β = $2 - f + f^2 2\omega_i\tau_i\omega_e\bar{\tau}$
Δ = shock detachment distance, m
ϵ = ionization distance, m; see Ref. 10 for precise definition
θ = angular coordinate measured from the magnet centerline, rad
ρ = fluid density, kg/m³
$\bar{\sigma}$ = tensor electrical conductivity, mho/m
σ_{eff} = effective electrical conductivity, mho/m
σ_0 = scalar electrical conductivity, mho/m
τ = electron-ion collision period, sec
τ_e, τ_i = electron-neutral, ion-neutral collision period, sec
$\bar{\tau}$ = $(\tau^{-1} + \tau_e^{-1})^{-1}$ mean collision period, sec
ω = (eB/m) cyclotron frequency, sec⁻¹

Subscripts

b = body
$\mathfrak{L}$ = centerline
e = electron
i = ion or "induced"
s = at shock
∞ = fluid upstream of shock
NM = no magnetic field present

Received May 9, 1963; revision received January 2, 1964. This work was partially sponsored by the Flight Control Laboratory, Aeronautical Systems Division, Air Force Systems Command U. S. Air Force, Wright-Patterson Air Force Base, Ohio under contract AF33(616)-7745, Project 8219, Task 821902. The authors are indebted to W. Evans for vehicle performance information, to Caryl Amon for her IBM programming work, and finally to R. A. Scheuing, Assistant Director of Research, and S. N. Milford, Head of Astrophysics, for their review and valuable criticism.

* Staff Scientist, Research Department.
† Research Engineer, Research Department. Member AIAA.

Introduction

CAN "onboard" magnetic fields interact with ionized flow to supply forces sufficient to control hypersonic vehicles? If so, what are the altitude and velocity ranges in which such control can be obtained? These questions have been made more pertinent by the discovery of high-field strength superconducting magnets, which require only the power necessary to maintain the cryogenic environment, and by the fact that future interplanetary vehicles may have onboard magnetic fields for protection from the charged particle radiation or for heat shielding against the high thermal loads on reentering the atmosphere. Furthermore, the potentialities for such new control techniques deserve consideration because of the difficulties encountered at hypersonic velocities with the usual means of aerodynamic control, i.e., by changing the shape of the vehicle.

MHD control requires no modification of the exterior vehicle geometry. Instead, forces act at a distance. The magnetic field is like an invisible porous flap that extends into the flow interacting with the ionized fluid and, in turn, producing a reaction at its source—the magnet on board the vehicle. This force is then transferred to the vehicle, producing the control moment. The general features can be seen in Fig. 1 where the nose region of a high-velocity vehicle is sketched for the situation at the beginning of a control maneuver with the electromagnet swiveled to an angle of attack. The high-temperature ionized shock layer is the electrically conducting fluid upon which the MHD control forces are exerted.

The analysis that follows begins with some of the fundamental equations of MHD that are utilized to develop a general expression for the MHD control force. It is demonstrated that the control force is proportional to a magnetic interaction parameter Q' and that the value of Q' must be of the order of 1 or greater for the force to be effective. Applicable velocity-altitude regimes are graphed. Once the strong interaction altitude-velocity region is known, it is then possible to estimate the control forces; these are presented both as forces and as dimensionless ratios of the control force to a characteristic aerodynamic force.

Aeronautical applications of MHD have been previously investigated. In his dissertation Patrick[1] looked into the possibilities of a hypersonic MHD generator. Resler and Sears[2] suggested the use of a magnetic field in the vehicle nose as a control device. Kantrowitz[3] has presented in a summary article an estimate of flight regimes in which a self-excited MHD generator "brake" would be feasible. It is interesting that his MHD brake regimes cover a much larger area than the MHD control regimes described in the following pages.

The strong interaction and MHD flight control regimes computed from the present analysis take account of and, in fact, make use of the changes produced by various "on-board" magnetic fields on the ionized shock-layer flow. To the authors' knowledge this is the first time that the results of such calculations are presented. These calculations must and do treat the conductivity as a tensor and include the magnetic fields induced by the shock-layer currents. A very important part of the analysis is the evaluation of the shock detachment distance, which sometimes can be enormous.

It should be kept in mind that both the difficulty and nature of the problem necessitate an order-of-magnitude approach. The analysis is concerned with the gross effects of the flow and the justification of the assumptions made. The results reported are not restricted to any specific class of vehicles; the only limitation is that the vehicle have a roughly spherical nose.

An over-all evaluation of MHD control would have to take into account various engineering problems, such as the switching and control of the magnetic field, component weights, the total system design requirements, and comparisons with alternate systems such as jet controls. Such considerations are beyond the scope of the present paper, which simply delineates the possible regions of MHD nose control and provides estimates of the necessary sizes and strengths of magnetic fields in these regions.

Theoretical Analysis and Results

Basic Equations

The basic equations that are used to evaluate the Lorentz (or MHD) forces acting on the ionized fluid are

$$\mathbf{F} = \int_\tau \mathbf{j} \times \mathbf{B} d\tau \tag{1}$$

and

$$\mathbf{j} = \bar{\sigma}(\mathbf{E} + \mathbf{u} \times \mathbf{B}) \tag{2}$$

In the continuum flight regimes being considered, it is appropriate to use this macroscopic formulation. Equation (1) is the expression for the force itself whereas Eq. (2) is the familiar Ohm's law, where $\bar{\sigma}$ is a tensorial conductivity strongly dependent upon the strength of the magnetic field. In the altitude-velocity regimes pertinent to MHD control, the tensor character of the conductivity is extremely important. To simplify the analysis, the flow behind the shock is divided into a symmetrical flow about the centerline of the applied B field $\mathbf{u}_{sym}$ and the crossflow component $\mathbf{u}_\alpha$ which is, in general, perpendicular to the B field. With reference to the configuration shown in Fig. 1, the currents that are due to the symmetrical portion of the flow through the B field form closed circular loops about the centerline of the B field‡ and exert an over-all unidirectional force on the fluid along $u_\infty \cos\alpha$, tending to push the shock away from the body. The currents, primarily responsible for the control forces, are produced by the crossflow of the ionized fluid through the B field. The angle α, between the centerline of the B field and the incoming flow, is assumed to be sufficiently small, so that the flow in the hemispherical nose region is not significantly affected by the afterbody.

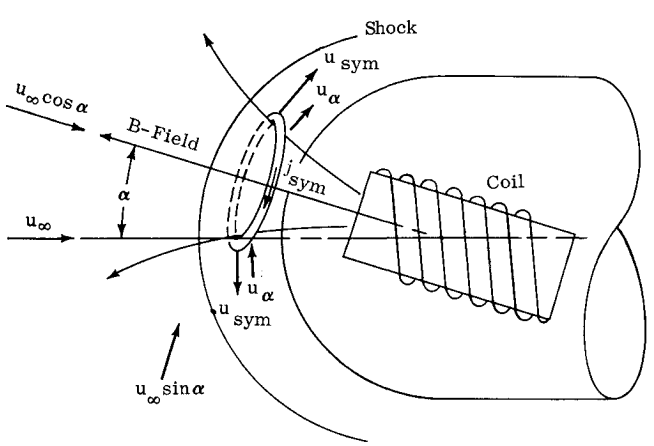

Fig. 1 Initial MHD control configuration with a B field at an angle of attack to the freestream.

Control Force Ratio f_M

From Ohm's law, Eq. (2), one may write the relation

$$\mathbf{j}_\alpha = \sigma_{\text{eff}}(\mathbf{E}_\alpha + \mathbf{u}_\alpha \times \mathbf{B}) \tag{3}$$

where $\mathbf{j}_\alpha$ is that part of the current density that is directed along $\mathbf{u}_\alpha \times \mathbf{B}$, and σ_{eff} is the effective conductivity of the current path in this direction. The electric field $\mathbf{E}_\alpha$ is the component of the electric field generated by the crossflow that is directed oppositely to $\mathbf{u}_\alpha \times \mathbf{B}$. (See Appendix for the derivation.) The electric field $\mathbf{E}_\alpha$ has a magnitude that depends upon the possible return current paths. If there are no return paths, $\mathbf{j}_\alpha = 0$ and $\mathbf{E}_\alpha = -\mathbf{u}_\alpha \times \mathbf{B}$. If a very highly conducting path exists on the surface or within the vehicle, the currents are short circuited, making $\mathbf{E}_\alpha \approx 0$ and $\mathbf{j}_\alpha \approx \sigma_{\text{eff}}(\mathbf{u} \times \mathbf{B})$. The possibility exists, of course, of placing electrodes along the sides of a crossflow through a B field and using the generated electric field and associated electrical power to produce the very same B field (a self-excited generator). Donaldson[4] did consider such a scheme in the afterbody region of a vehicle. He found it necessary to ionize the flow artificially with some seed material. A severe limitation to the use of a seeded side-flow, in comparison to the use of the shock-ionized fluid at the nose, is the relatively small amount of ionized fluid available. (It will be seen later that a B field can increase greatly the volume of the shock-layer flow.)

For purposes of this order-of-magnitude study, the average value of $\mathbf{E}_\alpha$ is assumed to be one-half the average value of the magnitude of $\mathbf{u}_\alpha \times \mathbf{B}$. With this assumption, the substitution of $\mathbf{j}_\alpha$ into Eq. (1) provides, in nondimensional form, the following approximate expression for the magnetic control-force ratio:

$$f_M = F_M/q_\infty A_b = Q'\bar{u}_\alpha/u_\infty \tag{4}$$

In this equation, F_M is the magnetic control force, $\bar{u}_\alpha$ is the appropriately averaged crossflow velocity perpendicular to $\mathbf{B}$, and

$$Q' \equiv \frac{1}{A_b}\int_\tau \frac{\sigma_{\text{eff}}B^2}{\rho_\infty u_\infty} d\tau \tag{5}$$

is the magnetic interaction parameter computed over the volume of the ionized fluid interacting with the magnetic field. Aerodynamic means of nose control, if made operable, could provide control forces of the order of 0.1 $q_\infty A_b$ for a flap of roughly the same frontal area as the nose. At the higher altitudes where the aerodynamic means of control become ineffective, the ratio f_M loses its significance, and the control force F_M becomes the more meaningful quantity.

Interaction Parameter Q'

It should be recognized that F_M is a resistive force, which opposes the crossflow. For Eq. (4) to be consistent with this fact, an increase in Q' must result in a larger f_M and a smaller $\bar{u}_\alpha$. Thus Q' gives a measure of the interaction be-

‡ Hall currents are omitted from the present discussion, since their magnitudes are assumed negligible in comparison to the currents described. This simplification is discussed in the section titled "Interaction Parameter Q'" and in the Appendix.

tween the fluid and the magnetic field. The value of Q' which separates regions of significant interaction from those where the interaction with the fluid is probably too small for control purposes may be taken as unity. A Q' of unity makes the force ratio equal to $\bar{u}_\alpha/u_\infty$, which is of the order of 0.1. For force ratios substantially less than 0.1, the interaction will not significantly affect the flow in the ionized shock layer; it will simply be a perturbation to the aerodynamic flow. For values of $Q' > 10$, a very strong interaction is to be expected.

Before proceeding to the problem of determining whether there are altitude flight regimes in which Q' is large, note that a characteristic length which can be associated with Q' is the shock detachment distance Δ. If $\sigma_{\text{eff}}B^2$ is treated as a constant average value, and if the volume of ionized flow is approximated by ΔA_b, then Q' [Eq. (5)], becomes

$$Q' \approx \frac{1}{A_b}\frac{\sigma_{\text{eff}}B^2\Delta A_b}{\rho_\infty u_\infty} = \frac{\sigma_{\text{eff}}B^2\Delta}{\rho_\infty u_\infty} \tag{6}$$

which shows Q' to be essentially an interaction parameter based upon the detachment distance. Note that throughout this investigation it will be assumed that the shock has a blunt shape similar to that of the body and that the region between the shock and the body is filled by the conducting gas. For very large Δ, Eq. (6) will underestimate Q', since the ionized volume will then exceed ΔA_b.

In the present work, Q' is evaluated by numerical integration of Eq. (5). In order to accomplish this operation one must know the effective electrical conductivity, magnetic field, detachment distance, and the volume of ionized fluid surrounding the nose of a hypersonic vehicle.

Effective Electrical Conductivity

Starting from a generalized current equation, such as that given by Cowling,[5] and assuming strong interaction, i.e., $\nabla p = \mathbf{j} \times \mathbf{B}$, the conductivity component in the $\mathbf{u} \times \mathbf{B}$ direction, which was identified with the subscript "effective," can be shown to be (see Appendix):

$$\sigma_{\text{eff}} = \frac{\sigma_0(2-f)(\beta^2 + k\omega_e^2\bar{\tau}^2)}{\beta(\beta^2 + \omega_e^2\bar{\tau}^2)} \tag{7}$$

where $\beta = 2 - f + f^2\omega_i\tau_i\omega_e\bar{\tau}$, in which f denotes the fraction of nonionized atoms. The averaged collision-period values $\bar{\tau}$ are conveniently obtainable from Ref. 6. An expression for τ_i is derived in Ref. 7.

The parameter k indicates the extent to which the Hall current has been restrained by charge polarization; $k = 1$ corresponds to zero Hall current, while $k = 0$ corresponds to unrestricted Hall currents. The effects on σ_{eff} of varying k between zero and 1 are demonstrated in Fig. 2 for a flight velocity of 8.5 km/sec. As expected, the highest effective conductivities appear for zero Hall current ($k = 1$). However, at the higher altitudes (80 km or higher for this particular velocity), β^2 strongly predominates; when this happens the conductivities become insensitive to the value of k. Of course, this insensitivity to k is also present at low altitudes, where the conductivity is effectively a scalar quantity: $\sigma_{\text{eff}} = \sigma_0$. The calculations herein are based on the $k = 1$ approximation. It will be recognized from Eq. (7) that, even with $k = 0.5$, the conductivities never fall below one-half the optimum values for $k = 1$. Figure 2 illustrates how close the effective conductivity values are for $k = \frac{1}{2}$ and $k = 1.0$.

The scalar electrical conductivities of normal-shock-ionized air have been computed assuming thermal equilibrium, zero heat transfer, and immediate ionization behind the shock. These values are used in the computation of the effective conductivities along the centerline of the B field. The assumptions involved are justified in the MHD flight-control regimes presented in this paper. Further discussion on the limitations of the assumptions can be found in Ref. 7.

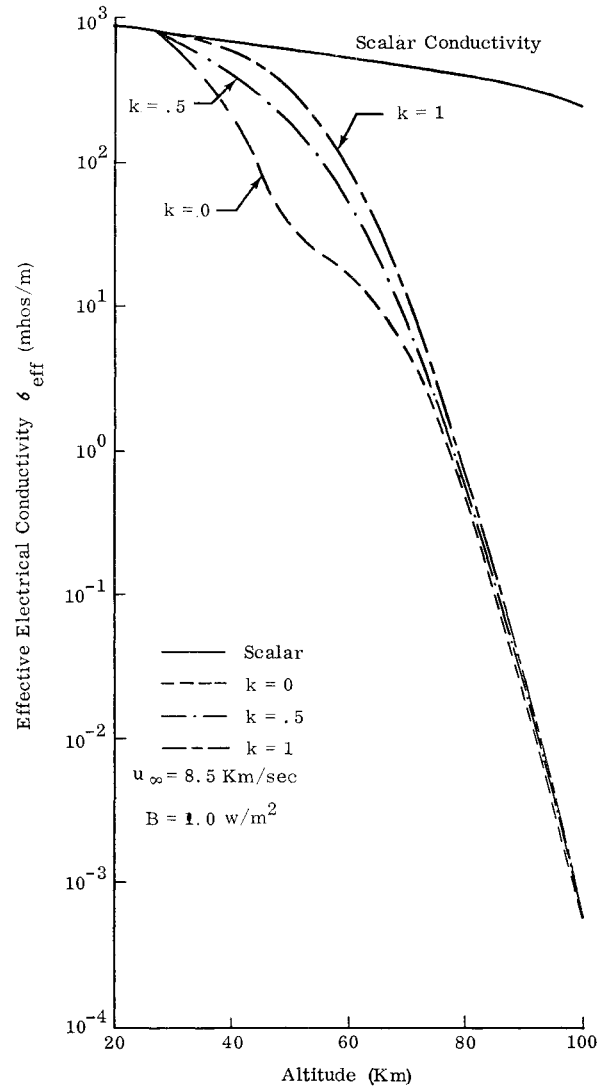

Fig. 2 Effective electrical conductivity behind normal shock in air for various values of Hall current parameter k.

Magnetic Field Distribution

For the B field, a dipole distribution is assumed to produce an applied field having a given value B_0 at the nose of the body. At superorbital flight velocities this distribution must be corrected for the induced field generated by the currents in the shock layer. Considering that the shock detachment distance is initially unknown, it might seem like a hopeless task to make the adjustment. It is accomplished in the IBM program, however, by means of multiple iterations, which, fortunately, converge fairly rapidly. The induced field calculations take into account the local variation of the effective electrical conductivities and use average shock-layer velocities as determined from conservation of mass.

Shock Detachment Distance

The determination of the detachment distance is one of the critical points in this investigation; it is based upon Bush's[8] analysis or, rather, what might be called a liberal interpretation of his analysis, as well as on an independent argument for the maximum value of the shock-front interaction parameter,

$$Q_s = \frac{\sigma_{\text{@}}B_s^2,_{\text{@}}r_s}{\rho_\infty u_\infty}$$

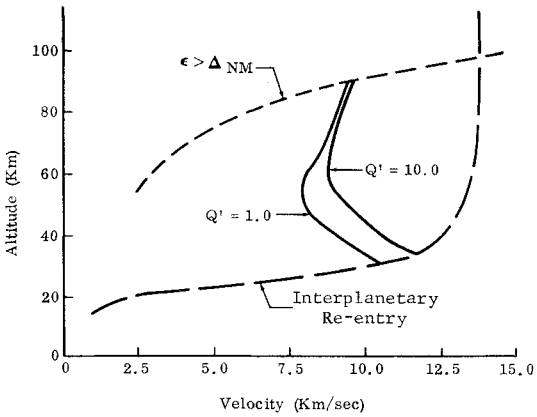

Fig. 3 Interaction parameter Q' for r_b = 0.5 m and B_0 = 1.0 Weber/m².

Using an electromagnetic shock tube, Ziemer[9] obtained experimental results which were in general agreement with Bush's work for values of Q_s which were not too large. Bush could not find solutions for values of Q_s greater than a certain critical value. This critical value is interpreted by the present authors as the maximum possible Q_s for the chosen density ratio. When Q_s is at its maximum value, any increase in B at the body will cause the shock to move further out, holding the limit on Q_s.

That there should be a maximum value of Q_s and that this value should be of the order of Bush's critical value, 17, follows from simple physical considerations. The momentum equation along a streamline near the shock front is, assuming $\mathbf{E} = \mathbf{u} \cdot \mathbf{B} = 0$,

$$\frac{\partial}{\partial s}\left(\frac{u^2}{2}\right) = -\frac{1}{\rho}\frac{\partial p}{\partial s} - \frac{\sigma u B^2}{\rho} \tag{8}$$

For strong magnetic interaction, the left-hand side of the foregoing equation approaches zero. For this situation it follows that over the interaction length ($\approx r_s$) the average pressure term will have to balance the average magnetic interaction term, i.e.,

$$-\overline{(\partial p/\partial s)} \approx \overline{\sigma u B^2} \tag{9}$$

For the magnitude of the pressure term, it is reasonable to take

$$-\overline{(\partial p/\partial s)} = k_1'(p_s/r_s) = k_1(\rho_\infty u_\infty^2/r_s) \tag{10}$$

where k_1' or k_1 is a number of the order of but less than 1 (with no interaction $k_1 \approx 1$, but for strong interaction k_1 is smaller), and p_s is the static pressure immediately behind the normal shock, which from the momentum jump condition is approximately $\rho_\infty u_\infty^2$. For the magnetic interaction

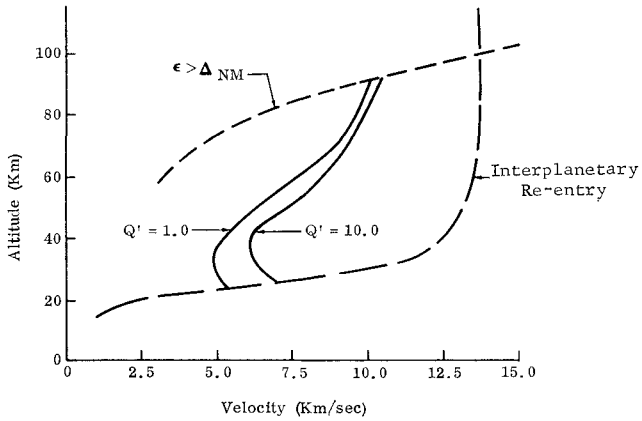

Fig. 4 Interaction parameter Q' for r_b = 0.5 m and B_0 = 10 Webers/m².

term, it is reasonable to set

$$\overline{\sigma u B^2} = k_2 \sigma_{\text{¢}} u_n B_{s,\text{¢}}^2 \tag{11}$$

where $\frac{1}{4} < k_2 < 1$ and $u_n = u_\infty \rho_\infty / \rho$. This last equation is consistent with the assumption of strong interaction where the velocity and conductivity do not strongly vary in the ionized subsonic part of the shock layer; e.g., assuming $\sigma = \sigma_{\text{¢}} \cos\theta$ and $u = u_n \tan\theta/\cos\theta$, $0 < \theta < \pi/3$, k_2 is computed to be 0.36. Substitution of Eqs. (10) and (11) into (9) gives

$$Q_{s_{\max}} = (k_1/k_2)(\rho/\rho_\infty) = k(\rho/\rho_\infty) \tag{12}$$

where $k = k_1/k_2$ is of order 1. Bush used 11 for ρ/ρ_∞ and his maximum possible interaction parameter at the shock turned out to be 16.8, indicating a k of approximately 1.5. This prediction is in agreement with our estimate that k should be of order 1.

Interaction Volume

An order of magnitude estimate of the interaction volume can be made, based on the following two considerations: 1) in hypersonic flow the subsonic cap extends to roughly $\theta = 30°$; and 2) with strong magnetic interaction, the flow acceleration in the shock layer will be appreciably retarded, so that the shock will be pushed out and the sonic line will shift. Just how great this shift in the sonic line will be, and how far into transonic region reasonably high electrical conductivities will extend, is not known (work in progress at Avco and Cornell Aeronautical Laboratories should provide some clarification on this subject), but one can expect that the stronger the interaction, the greater will be the displacement of the sonic line, provided the shock shape remains blunt. It is estimated that for strong magnetic interaction the ionized cap will extend to an average of 60° past the centerline of the B field.

Large Interaction ($Q' > 1$) Flight Regimes

The region over which we integrate to obtain Q' [Eq. (5)] is that region enclosed by the shock wave (assumed concentric with the body), the body nose, and a 120° cone with the vertex at the center of the nose curvature. Using spherical coordinates and assuming the B field and the effective conductivity to vary as the cosine of the angle θ, the following expression is obtained:

$$Q' = \frac{2\pi}{\pi r_b^2}\int_{r_b}^{r_s}\int_0^{\pi/3} \frac{\sigma_{\text{eff}\text{¢}}(r) B_{\text{¢}}^2(r) r^2 \cos^3\theta \sin\theta d\theta dr}{\rho_\infty u_\infty} \tag{13}$$

It is important to assay the uncertainty of the Q' calculations before discussing the results. The integral with respect to the angular variation $\int \cos^3\theta \sin\theta d\theta$ is almost linearly proportional to the limits for limiting angles $\leq \pi/3$. This means that, even if the actual interaction volume were to extend only to an average angular spread of 30°, the resulting Q' would be reduced by a factor of 2. The same conclusion can be reached concerning the dependence of Q' on the assumed angular variation of the electrical conductivity. Changing the exponent of the cosine in the conductivity expression from 1 to −2 or from 1 to +3 again changes the result by about a factor of 2. The −2 exponent corresponds to the strongly tensorial region, whereas +3 represents an overly large falloff in the scalar conductivity region. The integral over the radial variation is also seen to be only moderately sensitive to the shock detachment distance, which, in turn, weakly depends on the choice of the maximum Q_s. In practically all cases of large Q', $Q \gg Q_s$ within the shock layer. Therefore, it can be expected that the computed Q' values are of the right order of magnitude.

The altitude-velocity regimes for which $Q' = 1.0$ and $Q' = 10.0$ have been calculated and are shown in Figs. 3–5. Allowing for the uncertainties in the assumptions, one can

state: Regimes in which $Q' < 1$ are unfavorable, whereas those with Q' above 10 meet the strong interaction prerequisite for MHD flight control. The region between $Q' = 1$ and $Q' = 10$ is questionable. In addition to the constant Q' lines, these plots also display an interplanetary re-entry trajectory, which is typical for re-entry into the earth's atmosphere from an interplanetary mission, and a line above which the ionization distance ϵ is larger than the nonmagnetic shock detachment distance Δ_{NM}. Unless some artificial means were employed to establish initially a Δ much larger than Δ_{NM}, this curve of $\epsilon > \Delta_{NM}$ could constitute an upper bound on MHD control, because for greater altitudes the shock layer would not be ionized. The data for ϵ were taken from Teare, as reported by Feldman.[10]

Figure 3 shows that, for a nose radius of 0.5 m and a magnetic field at the stagnation point B_0 of 1.0 Webers/m^2, the velocities favorable to MHD control are in excess of about 8 km/sec. The effect of increasing the B field to 10 Webers/m^2 is evident from Fig. 4, where the favorable velocities start at approximately 5 km/sec. Figure 5 shows an extreme example of a large body and a large magnetic field ($r_b = 5.0$ m and $B_0 = 10$ Webers/m^2). As might be expected, the MHD control is more favorable with larger body dimensions; large interactions are indicated for velocities as low as 3.5 km/sec.

It is of interest to note how p varies with Q' for a given altitude and flight speed. This connection is shown in Fig. 6 for a body with a nose radius of 0.5 m. The variation in Q' is effected here by changing the applied magnetic field strengths. Both Q' and p are shown to increase to very large values with increasing B_0.

Force Expression for Large Q'

As pointed out in the section titled "Interaction Parameter Q'," a large Q' means that a substantial interaction takes place, and because of this, $\bar{u}_\alpha/u_\infty$ in the force ratio expression [Eq. (4)] is a very small quantity approaching zero as Q' increases. Under these circumstances the magnetic force F_M will, to a good approximation, simply equal the total rate of momentum change of the freestream crossflow which is effectively stopped by the increased detachment distance

$$F_M = \rho_\infty u_\infty^2 \sin^2\alpha A_c \tag{14}$$

where A_c is the increase in the cross-sectional area of the shock layer brought about by the magnetic increase in shock detachment distance, and α is the angle between the centerline of the B field and incoming flow. For the purposes of the present calculations, the crossflow in the shock layer is assumed to be stopped by the presence of the B field, and the stagnation streamline to have shifted toward the centerline of the B field.

Assuming again an average angular spread of $\pi/3$ rad for the ionized subsonic region that is entrapped on either side of the centerline of the B field, one finds the value of A_c to be given approximately by

$$A_c \simeq \frac{2\pi}{3} r_b^2 (p - p_{NM}) \left(1 + \frac{p}{2}\right) \tag{15}$$

Neglecting p_{NM} with respect to p (p is much larger than p_{NM} for large Q') and substituting (15) in (14) and again nondimensionalizing with respect to the rate of freestream momentum at the nose, the following expression is obtained for the magnetic force ratio

$$f_M = \tfrac{2}{3} \sin^2\alpha\, p(2 + p) \tag{16}$$

A conservative estimate of the values of p to be inserted in the foregoing formula is that obtained for zero angle of attack flow. This value is conservative on two counts: first, the momentum in the direction of the centerline of the B field is less than that along the axis of the body (therefore, less normal momentum for the B field to stop), and second, the presence of the crossflow through the B field adds to the pressures in the shock layer pushing out the shock.

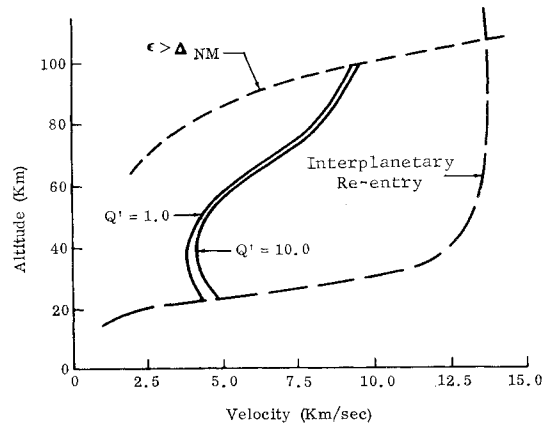

Fig. 5 Interaction parameter Q' for $r_b = 5.0$ m and $B_0 = 10$ Webers/m^2.

MHD Flight Control Regimes

The force ratios f_M and the total MHD control force F_M for several magnetic field configurations are presented in Figs. 7–9. All of these results are for one body radius, $r_b = 0.5$ m, and a 30° angle of the magnet with the freestream. The optimum magnet angle could well be greater, but the choice of an angle substantially larger than 30° would be incompatible with the small angle assumptions. A force ratio of 0.1 is considered a lower limit for the usefulness of nose control applications. With reference to these figures, regimes to the right of $f_M = 0.1$ and below the upper bound $\epsilon = \Delta_{NM}$ are designated as MHD flight-control regimes.

The constant f_M envelopes for a B_0 of 10 Webers/m^2 is shown in Fig. 7. It is evident that, for an interplanetary re-entry vehicle, there exist significant control regimes extending down to an altitude of 30 km and a speed of 6 km/sec. When the magnetic field is reduced to 1 Weber/m^2 (Fig. 8), there still remains an important region of control. It is apparent,

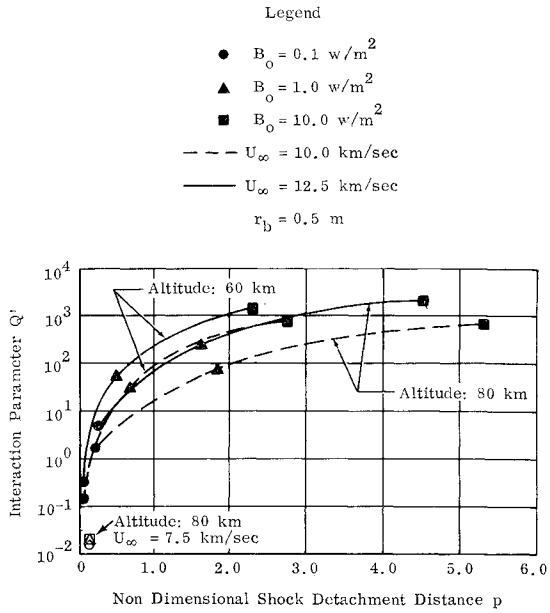

Fig. 6 Variation of shock-layer interaction parameter Q' and nondimensional detachment distance p with increments of B_0 for given flight speed and altitude (the radius of the nose is taken as 0.5 m).

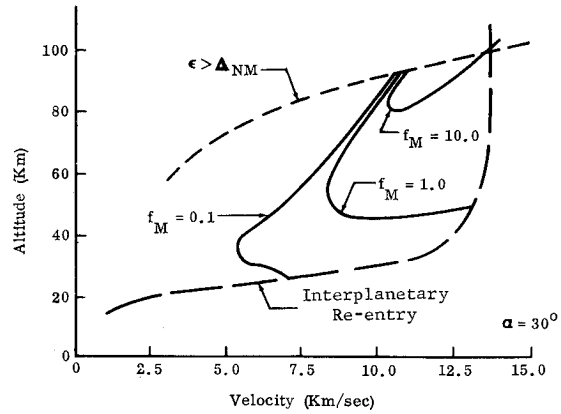

Fig. 7 Magnetic control force ratio f_M for r_b = 0.5 m and B_0 = 10 Webers/m².

however, that supersatellite velocities are required in order to achieve feasible f_M ratios.

Values of F_M corresponding to 10 Webers/m² are shown in Fig. 9. It will be noticed that control forces in excess of 10^4 N (2250 lb) can be expected in certain flight regimes.

Experimental results on a representative hypersonic body to which the results of the present paper can be applied (for M_∞ = 9.6) were obtained in Ref. 11, and the computed results based on these data are presented in Fig. 10. (In the hypersonic regime the dependency of the trim force coefficient on the Mach number is weak.) The force coefficient needed to trim may be compared directly with the available MHD force coefficient f_M. A rough comparison indicates that the values of f_M for supersatellite velocities are of the same magnitude as the trim force coefficients required for this representative body at moderate vehicle angles of attack.

Summary and Conclusions

Using an analysis based on certain plausible but incompletely verified assumptions, it has been deduced that a necessary condition for MHD nose control is a large value of an interaction parameter Q', which is essentially based upon the shock detachment distance. Velocity-altitude regimes characterized by large Q's ($Q' > 1$) have been determined; these represent regions where the MHD forces significantly affect the flow. As demonstrated in Figs. 3–5, the regimes of large interaction extend upward from flight velocities roughly equal to satellite velocity, and thus would accommodate the major portion of interplanetary re-entry or similar trajectories. Flight regimes where the computed MHD force ratios are larger than 0.1 (MHD flight-control regions) are presented in Figs. 7 and 8 for a body nose radius of 0.5 m.

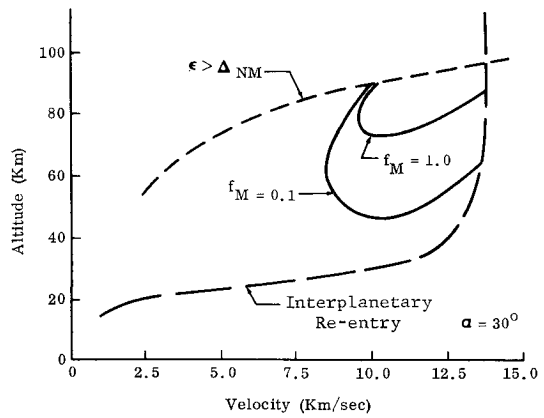

Fig. 8 Magnetic control force ratio f_M for r_b = 0.5 m and B_0 = 1.0 Weber/m².

The control scheme considered uses the shock ionized flow in the nose region and requires no seeding. The conditions for MHD flight control were found to improve greatly with increasing speed and magnetic field strength. Increasing the body nose dimensions widens the favorable altitude and velocity range. Within the range of the small magnet angles considered, the control force increases with $\sin^2\alpha$ [see Eq. (16)]. The MHD control forces compare well with those necessary to trim a 20° blunt cone type of vehicle having a relatively small nose area.

Appendix: Derivation of the Effective Electrical Conductivity

The general current relation for a partially ionized gas is given by Cowling[5] as

$$n_e e\mathbf{E}' + \nabla p_e = (B/\omega_e\bar{\tau})\,\mathbf{j} + \mathbf{j}\times\mathbf{B} + (f^2/B)2\omega_i\tau_i\{(\nabla p_e - \mathbf{j}\times\mathbf{B})\times\mathbf{B}\} \quad \text{(A1)}$$

where $\mathbf{E}' = \mathbf{E} + \mathbf{u}\times\mathbf{B}$, and it is assumed that the gas is in thermodynamic equilibrium, thermal diffusion effects are negligible, and $\omega_e\tau_e \gg \omega_i\tau_i$.

The electron pressure term is estimated with the aid of the momentum equation applied within the shock layer

$$\rho/(D\mathbf{u}/Dt) = -\nabla p + \mathbf{j}\times\mathbf{B}$$

For very strong MHD interactions, the inertial term will be relatively unimportant and $\nabla p \approx \mathbf{j}\times\mathbf{B}$. Using the law of partial pressures and neglecting the variation in f,

$$\nabla p_e = \nabla\left(\frac{1-f}{2-f}\right)p \approx \left(\frac{1-f}{2-f}\right)\mathbf{j}\times\mathbf{B}$$

A lengthy but straightforward vector manipulation then yields a generalized Ohm's law in the form

$$\mathbf{j} = \frac{\sigma_0\beta(2-f)}{\beta^2 + (\omega_e\bar{\tau})^2}\left\{\mathbf{E}' - \frac{\omega_e\bar{\tau}}{\beta B}\mathbf{E}'\times\mathbf{B} + \left[\left(\frac{(\omega_e\bar{\tau})^2}{(2-f)\beta} + \frac{\beta}{2-f} - 1\right)\mathbf{E}'\cdot\mathbf{B}\right]\frac{\mathbf{B}}{B^2}\right\} \quad \text{(A2)}$$

where $\sigma_0 = n_e e^2\bar{\tau}/m_e$. Equation (2) in the text may be thought of as the symbolic form of (A2). The tensor character of the generalized Ohm's law is clearly evident in (A2), where $\mathbf{j}$ is not, in general, in the same direction as $\mathbf{E}'$.

To obtain the expression for the effective electrical conductivity, an orthogonal coordinate system x, y, z is selected, where $\mathbf{B}$ points in the z direction and y is taken in the direction of the imposed electric field (in this case y is in the direction of $\mathbf{u}\times\mathbf{B}$), and the numeric k is introduced: $k \equiv \beta E_x'/$

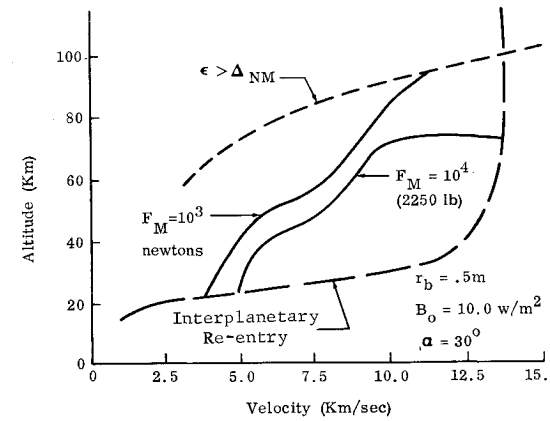

Fig. 9 MHD control force F_M for B_0 = 10 Webers/m² and α = 30°.

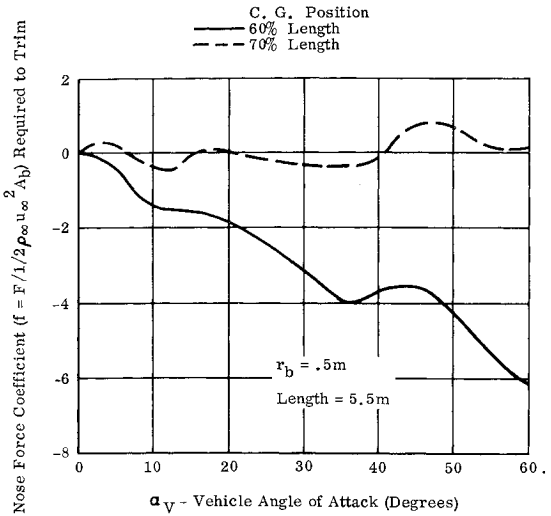

Fig. 10 20° blunt cone nose force coefficient required to trim.

$\omega_e\bar{\tau}E_y'$. With these choices the current density component in the direction of the imposed field can be written as

$$j_y = \frac{\sigma_0(2-f)(\beta^2 + k\omega_e{}^2\bar{\tau}^2)}{\beta(\beta^2 + \omega_e{}^2\bar{\tau}^2)} E_y' \equiv \sigma_{\text{eff}} E_y' \qquad \text{(A3)}$$

In the x direction, which is the direction of the Hall current,

$$j_x = \frac{\sigma_0(2-f)(k-1)\omega_e\bar{\tau}}{\beta^2 + \omega_e{}^2\bar{\tau}^2} E_y' \equiv \sigma_{\text{Hall}} E_y' \qquad \text{(A4)}$$

The right-hand side of Eqs. (A3) and (A4) define the effective conductivity and the Hall conductivity. It will be noted that, for $k = 1$, σ_{eff} reaches its maximum value of $\sigma_0(2-f)/\beta$ and no Hall current will flow; whereas at the lower limit of $k = 0$, σ_{eff} is reduced to $\sigma_0(2-f)\beta/(\beta^2 + \omega_e{}^2\bar{\tau}^2)$ and the Hall current reaches its maximum value. At the intermediate value $k = \frac{1}{2}$, σ_{eff} is never less than $\frac{1}{2}$ of σ_{eff} for $k = 1$, and the Hall currents are negligible. See Fig. 2 for influence of the numeric k on σ_{eff}.

References

[1] Patrick, R. M., "Magnetohydrodynamics of compressible fluids," Doctoral Dissertation, Cornell Univ. (June 1956).

[2] Resler, E. L., Jr. and Sears, W. R., "The prospects for magneto-aerodynamics," J. Aerospace Sci. **25**, 235–245, 258 (1958).

[3] Kantrowitz, A., "Flight magnetohydrodynamics," *Symposium of Plasma Dynamics*, edited by F. H. Clauser (Addison-Wesley Publishing Co., Inc., Reading, Mass., 1960), Chap. VII.

[4] Donaldson, C. and Gray, K., "Investigation of a magnetohydrodynamic channel for the control of high speed vehicles," Aeronautical Research Associates of Princeton Rept. 26, prepared for General Electric Co., Missile and Space Vehicle Div. (June 1960).

[5] Cowling, T. G., *Magnetohydrodynamics* (Interscience Publishers Inc., New York, 1957), Chap. VI, p. 107.

[6] Bachynski, M. P., Shkarofsky, I. P., and Johnston, T. W., "Plasma physics of shock fronts," Radio Corporation of America, Res. Rept. 7-801, AD245921 (June 1959).

[7] Ericson, W. B., Maciulaitis, A., Spagnolo, F. A., Scheuing, R. A., Loeffler, A. L., Jr., and Hopkins, H. B., Jr., "An investigation of magnetohydrodynamic principles applicable to flight control," U. S. Air Force, Aeronaut. Systems Div. Tech. Doc. ASD-TDR-62-649 (December 1962).

[8] Bush, W. B., "Magnetohydrodynamic-hypersonic flow past a blunt body," J. Aerospace Sci. **25**, 685–690, 728 (1958).

[9] Ziemer, R. W., "Experimental investigation in magneto-aerodynamics," ARS J. **29**, 642–647 (1959).

[10] Feldman, S., "On trails of axisymmetric hypersonic blunt bodies flying through the atmosphere," J. Aerospace Sci. **28**, 433–448, 470 (1961).

[11] Wells, W. R. and Armstrong, W. D., "Tables of aerodynamic coefficients obtained from developed Newtonian expressions for complete and partial conic and spherical bodies at combined angles of attack and sideslip with some comparisons with hypersonic experimental data," NASA TR R-121 (1962).